

# An Energy-Based Fatigue Model for Wrought Magnesium Alloy under Multiaxial Load

Jafar Albinmousa<sup>1</sup>, Hamid Jahed<sup>1</sup>, Steve Lambert<sup>1</sup>

<sup>1</sup> Fatigue and Stress Analysis Laboratory, Mechanical and Mechatronics Engineering Department, University of Waterloo, 200 University Ave. W., Waterloo, ON, N2L 3G1, CANADA; Tel: +1 519 888-4567 x37826; E-mail: [hjahedmo@uwaterloo.ca](mailto:hjahedmo@uwaterloo.ca)

**ABSTRACT.** *In automotive applications, load bearing components are subjected to multiaxial fatigue loading. Thus, a better understanding of multiaxial fatigue behaviour is a necessary step in the fatigue design of these components. This paper focuses on the cyclic behaviour of extruded AZ31B magnesium alloy. Flat and tubular specimens were machined from large AZ31B extrusion sections. Two loading modes were considered for multiaxial tests: tension and torsion. All tests were performed at standard laboratory and in as-received conditions. Cyclic axial test results indicate that AZ31B exhibit asymmetrical cyclic behaviour due to twinning. In contrast, cyclic torsional behaviour was found to be symmetric. Multiaxial proportional tension-torsion shows an overall asymmetric hysteresis. Energy is being considered as a potential fatigue parameter to correlate the tension, shear and multiaxial results. As a scalar valued function, there is no ambiguity in defining energy as an equivalent measure of damage at different material directions. Other equivalent measures such as strain, due to anisotropic characteristics of AZ31B, are not simply defined. Results of correlating axial, torsional and multiaxial proportional using an energy parameter are shown and discussed.*

## INTRODUCTION

Magnesium alloys are the lightest structural metal and have high specific strength and stiffness, which make them attractive for aerospace and automotive industries. However, load bearing structural components in automobiles are usually subjected to cyclic loading in a multiaxial manner. Thus, it is important to characterize and model the fatigue behaviour of these alloys under axial and shear cyclic loads.

Among magnesium alloys, wrought magnesium alloys have shown very good specific strength. There have been a number of reports on magnesium behaviour under monotonic [1, 2] and uniaxial cyclic loading [3- 10]. Due to the activation of the twinning mechanism [11], the cyclic tensile behaviour of the AZ31B extrusion was found to be qualitatively different from that of cyclic shear [12].

However, the multiaxial fatigue behaviour of Mg alloys has not been investigated. This is of particular importance because in practise components are

subjected to multiaxial loading. This paper presents the multiaxial fatigue behaviour of AZ31B extruded alloy. A cyclic total energy parameter is employed as a fatigue damage parameter to correlate the test results.

## MATERIAL

The investigated material in this analysis is an air-quenched AZ31B extrusion section that was prepared by Timminco and extruded from a 177.8 mm diameter by 406.4 mm long billet, with an extrusion ratio of 6. The extrusion temperature was between 360 and 382°C and the extrusion exit speed was 50.8 mm/s. The chemical composition is listed in Table 1.

Table 1. Chemical composition for extruded AZ31B (wt%)

Al	Mn	Zn	Fe	Ni	Cu
3.10	0.54	1.05	0.0035	0.0007	0.0008

## EXPERIMENTS

Two types of specimens, flat and tubular, were used for this investigation. All tests were performed at standard laboratory conditions using a servo hydraulic fatigue frame. Uniaxial and biaxial extensometers were used for axial and torsional strain measurements, respectively.

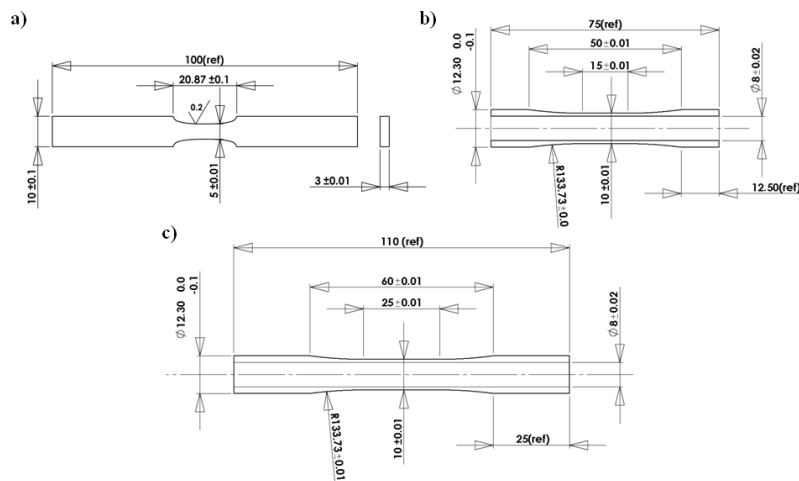


Figure 1. Specimen geometry and sizes, (a) flat specimen, (b) sub-sized tubular specimen used for compression test, and (c) full size tubular specimen; all dimensions in mm.

The geometries and sizes of the specimens are shown in Fig. 1. The flat specimens were machined in three different orientations, longitudinal (LD – parallel to the extrusion direction), transverse (TD), and at an angle of 45°. The monotonic torsion,

cyclic tension and torsion, and multiaxial tests were all performed on tubular specimens. Sub-sized tubular specimens were used for monotonic compression tests to avoid buckling. Fully reversed axial and torsional fatigue tests were performed under strain control with a sinusoidal waveform.

## MONOTONIC AND CYCLIC BEHAVIOUR

### *Monotonic*

The monotonic behaviour of the AZ31B extrusion is shown in Fig. 2. This figure shows the engineering stress strain curves for three monotonic tensile tests that were performed for the longitudinal, i.e., the extrusion direction, transverse and 45° directions. Also, this figure shows the compressive stress-strain curve for a specimen that was machined along the extrusion direction. It should be noted that this monotonic compressive test was stopped before failure. Therefore, the end point in the stress strain curve for the compression specimen is not the ultimate compressive stress. The monotonic shear stress-strain curve is also shown in this figure.

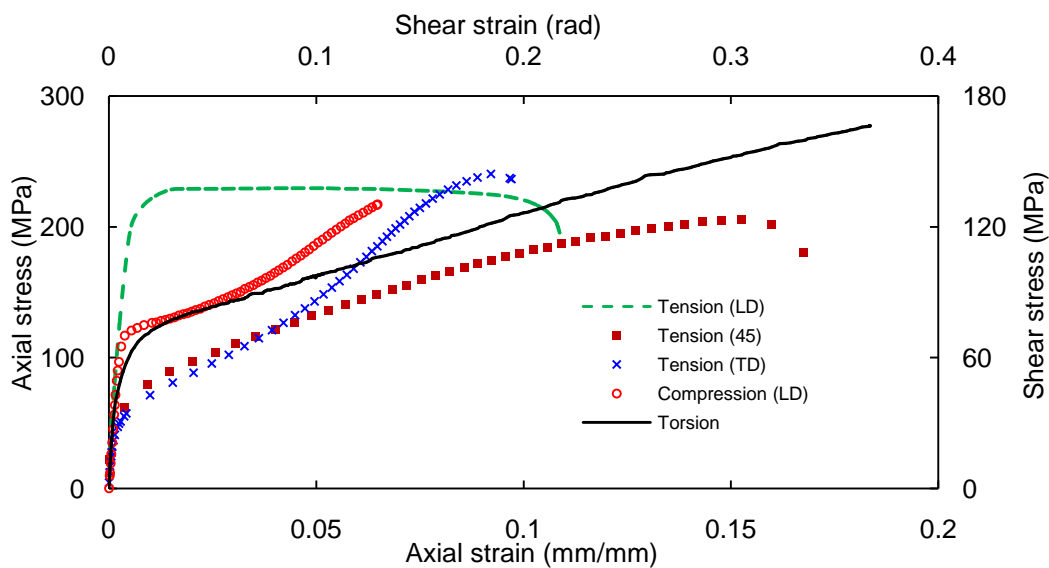


Figure 2. Monotonic tensile, compressive, and shear behaviour of AZ31B extrusion.

### *Cyclic*

Cyclic tests were performed for two loading conditions: pure tension and shear. The hysteresis loops for the first and the half-life cycles for pure cyclic tensile and shear loading are shown in Fig. 3. This figure demonstrates the asymmetric behaviour of AZ31B extrusions in cyclic tension, which is not observed in cyclic torsion. Also, the cyclic tensile hysteresis behaviour indicates that the AZ31B extrusion exhibits plastic strain recovery as the size of the half life hysteresis is seen to be smaller than that of the first cycle.

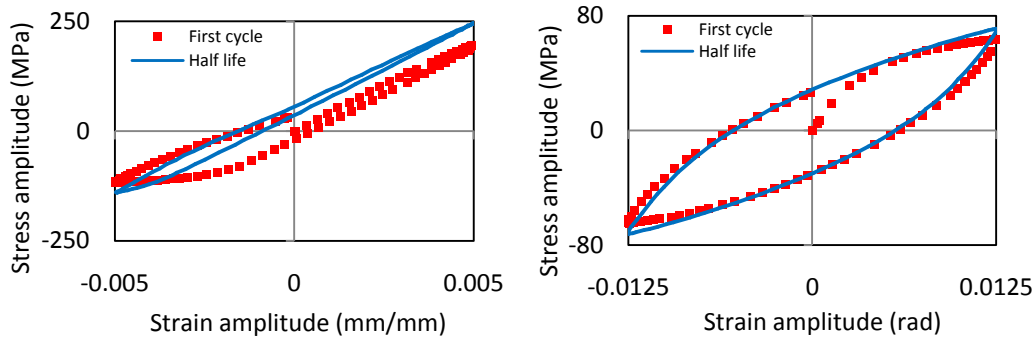


Figure 3. Pure cyclic tension,  $\epsilon_a = 0.5\%$ , (left) and torsion,  $\gamma_a = 1.25\%$ , (right) behaviour of AZ31B extrusion.

The tensile and shear strain life curves for pure cyclic tensile and shear tests are shown in Fig. 4. This figure shows the low cycle fatigue lives. The life ( $N$ ) was defined as the cycle at which the tensile or shear stress amplitude showed an abrupt drop. The general trend for the two loading modes indicates that the fatigue life increases linearly as the strain amplitude decreases.

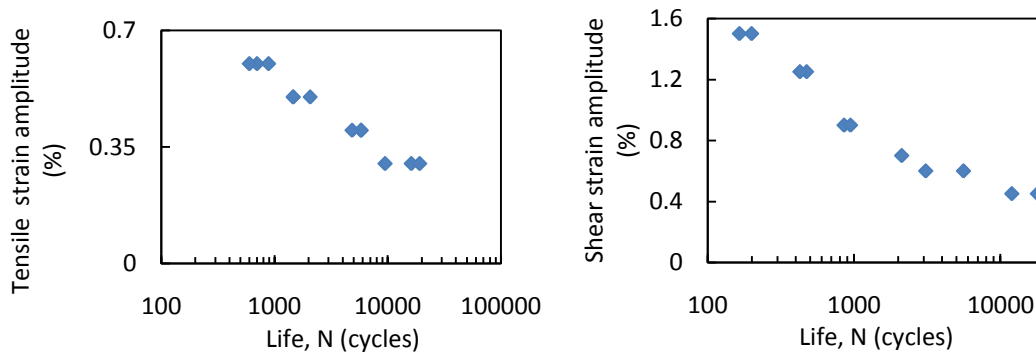


Figure 4. Tensile and shear strain life curves of AZ31B extrusion.

## MULTIAXIAL BEHAVIOUR

Three multiaxial tests were performed as listed in Table 2. The multiaxial proportional and nonproportional cyclic behaviour of the AZ31B extrusion is shown in Figs. 5 and 6, respectively. From these figures, it is seen that both the proportional and the nonproportional loading cases develop cyclic hardening. In the case of the proportional loading case, positive mean stresses in tensile and shear modes are observed. However, in the nonproportional loading case, negative shear mean stress is observed while the tensile mean stress is positive. Similar to pure cyclic tension, the cyclic tensile hysteresis for both proportional and nonproportional loading indicate plastic strain recovery, which is not observed in the shear mode. While the hysteresis behaviour in

pure cyclic shear is symmetric, multiaxial loading causes asymmetry in the cyclic shear hysteresis behaviour. However, this asymmetry seems to vanish with cycling as the half life hysteresis behaviour for the cyclic shear mode became symmetric in both the proportional and nonproportional cases. This change is mainly attributed to large plastic strain recovery in the compression cycle, leading to an increase in the compression yield value.

Table 2. Multiaxial test summary.

Specimen	$\varphi(^{\circ})$	$\varepsilon_a$ (%)	$\gamma_a$ (%)	$N$ (cycle)
BA-1	0	0.45	0.52	1050
BA-2	0	0.375	0.5	3740
BA-3	90	0.375	0.5	5800

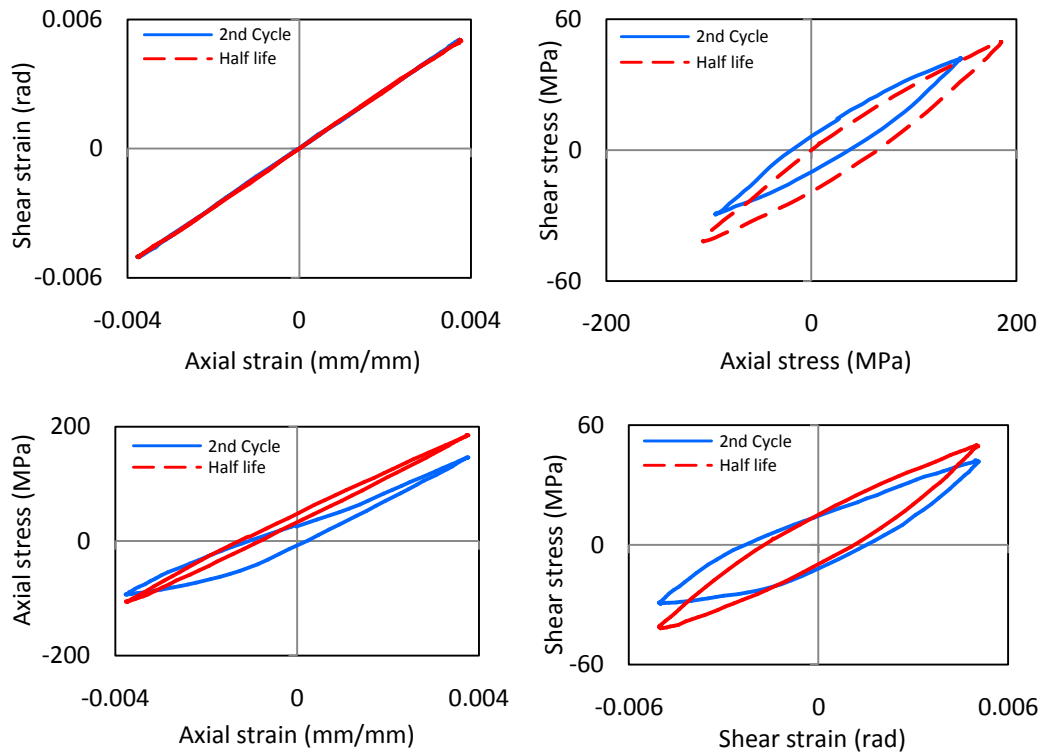


Figure 5. Multiaxial cyclic behaviour of the AZ31B extrusion. Proportional loading with amplitudes of  $\varepsilon_a = 0.375\%$  and  $\gamma_a = 0.5\%$ .

Two energies can be calculated from the cyclic hysteresis loop: plastic strain and elastic energies in the positive or negative quadrants. Because the tensile reversal is different than the compressive in pure cyclic tension, and to capture this difference, the total energy, defined as the sum of all energies (plastic and positive elastic), is considered here. The addition of the elastic energy allows the inclusion of the mean stress. In addition, the elastic energy helps avoid the problem associated with

calculating small plastic strain energies [13, 14]. Figure 7 shows the evolution of the total energy with cycling for different cyclic tests. In general, the total energy is either constant or increases linearly, with a shallow slope, with cycling.

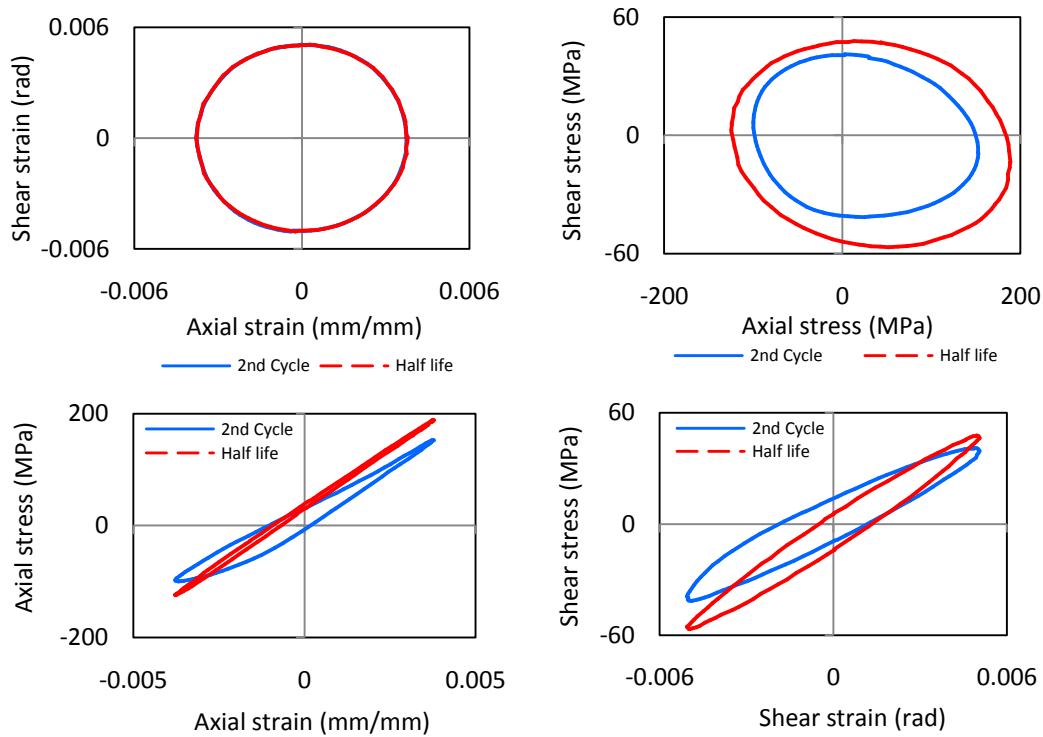


Figure 6. Multiaxial cyclic behaviour of the AZ31B extrusion. 90° out-of-phase nonproportional loading with amplitudes of  $\epsilon_a = 0.375\%$  and  $\gamma_a = 0.5\%$ .

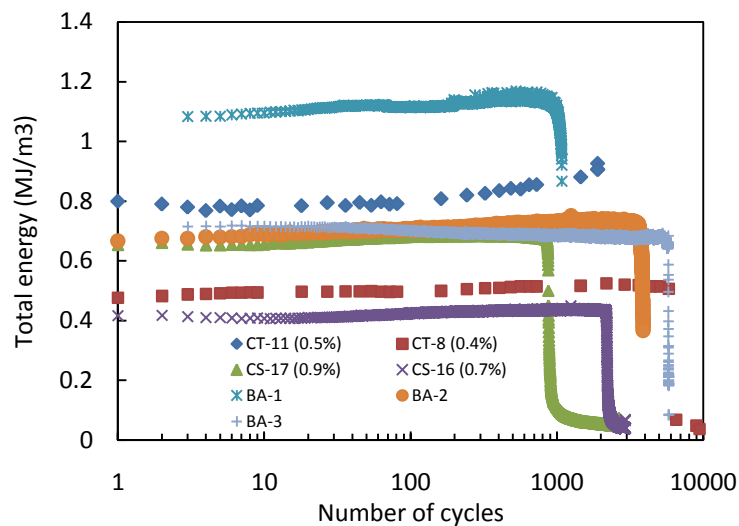


Figure 7. Total energy evolution with respect to number of cycle for pure tensile (CT) and shear (CS) and multiaxial (BA) cyclic tests. The abrupt drop is taken as the life.

## DAMAGE PARAMETER

Wrought magnesium alloys have shown strong directional properties and yield asymmetry. Any multiaxial fatigue parameter must accommodate this anisotropy. Correlation of strain or stress amplitudes as a function of loading path requires a complete anisotropic cyclic plasticity model. However, energy, being a scalar-valued function and hence load path independent, may be adopted as a multiaxial fatigue damage parameter without a need for further considerations. Due to the difference in the cyclic behaviour of AZ31B extrusion in tensile and shear modes, total energy is considered as a damage parameter here. The proposed damage parameter is plotted in Fig. 8 to correlate the test results. A fairly good correlation exists between many of the fatigue data obtained in cyclic tension-compression, cyclic torsion, and proportional tension-torsion.

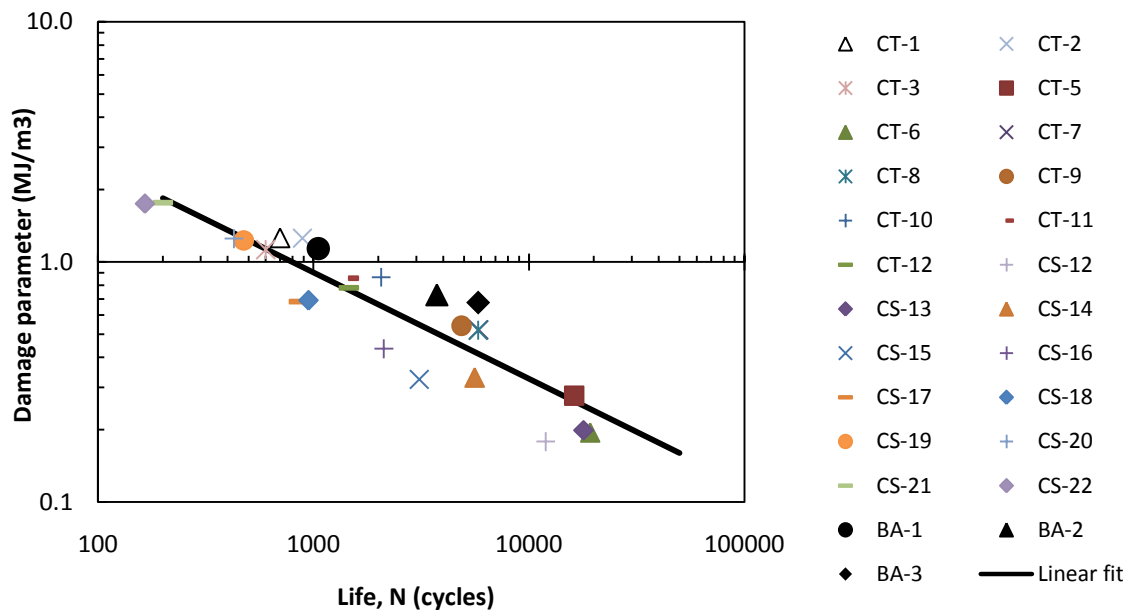


Figure 8. Total energy as a damage parameter vs. life for pure tensile (CT), shear (CS), in-phase and 90° out-of-phase multi-axial (BA) cyclic tests.

A line fitted through this correlation gives  $R^2 = 0.829$ , and establishes a fatigue-life relation given by Eq. 1:

$$\log D = m (\log N)^n \quad (1)$$

where  $N$  is the fatigue life,  $D$  is the proposed damage parameter, and  $m$  and  $n$  are the fatigue parameters. The parameters were found to be  $m = 20.5$  and  $n = -0.45$ .

## CONCLUSION

The multiaxial fatigue behaviour of extruded AZ31B alloy has been investigated. Cyclic tension-compression, cyclic torsion, proportional and 90° out-of-phase nonproportional tests were performed. The results obtained show that the fatigue lives from in-phase multiaxial and pure cyclic tensile and shear tests fall within the same scatter bands.

The total cyclic energy, i.e., plastic strain and positive elastic energies, was defined as a damage parameter. It was found that the fatigue data was well correlated using the proposed fatigue damage parameter. A promising fatigue-life model is therefore established.

## ACKNOWLEDGMENT

The authors acknowledge the support of AUTO21, the Natural Science and Engineering Research Council of Canada (NSERC), and the CANMET Material Testing Laboratory.

## REFERENCES

1. S. Kleiner and P. J. Uggowitzer (2004) *Mat Sci Eng A-Struct* **379**: 258-263.
2. Staroselsky and L. Anand (2003) *Int.J.Plast.* **19**: 1843-1864.
3. J. Albinmousa, H. Jahed, S. Lambert, S. Begum, D. Chen Q. Duan, T. Luo, Y. Yang, Z. Zhang, M.F. Horstemeyer, J. B. Jordon, A. Pascu A.A. Luo, R. Osborne, X. Su and L. Zhang (2010) *SAE world congress (In Press)*.
4. Brown D. W., Jain A., Agnew S. R. and Clausen B (2007) *Mater Sci forum* **539-543**: 3407-3413.
5. Lijia Chen, Chunyan Wang, Wei Wu, Zheng Liu, Grigoreta M. Stoica, Liang Wu and Peter K. Liaw (2007) *Metall Mater Trans A* **38**: 2235-2241.
6. S. Hasegawa, Y. Tsuchida, H. Yano and M. Matsui (2007) *Int.J.Fatigue* **29**: 1839-1845.
7. X. Y. Lou, M. Li, R. K. Boger, S. R. Agnew and R. H. Wagoner (2007) *Int.J.Plast.* **23**: 44-86.
8. S. Khan, Y. Miyashita, Y. Mutoh and Z. Bin Sajuri (2006) *Mat Sci Eng A-Struct* **420**: 315-321.
9. Z. Y. Nan, S. Ishihara, T. Goshima and R. Nakanishi (2004) *Scr.Mater.***50**: 429-434.
10. H. Zenner and F. Renner (2002) *Int.J.Fatigue* **24**: 1255-1260.
11. M. R. Barnett (2007) *Materials Science and Engineering A* **464**: 1-7.
12. J. Albinmousa, H. Jahed, S. Lambert (2010) *TMS Annual Meeting & Exhibition (In Press)*.
13. H. Jahed and A. Varvani-Farahani (2006) *Int.J.Fatigue* **28**: 467-473.
14. H. Jahed, A. Varvani-Farahani, M. Noban and I. Khalaji (2007) *Int.J.Fatigue* **29**: 647-655.